

MAGNETIC FLOW SORTING USING SUSCEPTIBILITY-MODIFIED CARRIER FLUIDS

L.R. Moore¹, P.S. Williams¹, J.J. Chalmers², & M. Zborowski¹

¹*The Cleveland Clinic Foundation, 9500 Euclid Ave. ND20, Cleveland, OH 44195, USA*

²*The Ohio State University, Columbus, OH 43210 USA*

INTRODUCTION: Continuous flow magnetic cell sorting with a Quadrupole Magnetic Flow Sorter (QMS) has been successfully applied to the isolation of cells of biological interest, and is particularly relevant to stem cell isolation. Specific cell populations are labeled with magnetic nanosphere-antibody conjugates, rendering them magnetic compared with non-binding negative cells. Our QMS device consists of an annular channel placed in the bore of a permanent quadrupole magnet, which generates a radial magnetic force. The theory specific to this system is validated by experiments with cells and calibration microspheres [1,2]. The positive cell recovery is predicted once the mobility distribution is known, with the aid of our novel device, the Cell Tracking Velocimeter (CTV). CTV generates mobility histograms of cell populations by sequentially tracking their motion in a well-characterized magnetic field [3].

Enriched fraction purities are difficult to predict and control. Due to a combination of flow non-idealities and geometric imperfections, negative cell “crossover” into the enriched fraction inevitably occurs in the QMS. Even a low fractional crossover can have a large impact when target cells are rare in the feed, as in the case of progenitor cells in apheresis product or umbilical cord blood. An attractive solution is the introduction of magnetic material into the carrier. Since transverse migration is governed by the difference in magnetic susceptibility between the cell and medium, raising the susceptibility of the medium has the effect of repelling the unlabeled - and therefore, non-magnetic - cells from the increasing magnetic field gradient, while only slightly retarding the motion of the magnetically-labeled cells.

The magnetic contrast agent, MAGNEVIST® (gadopentetate dimeglumine) (Berlex Laboratories, Wayne, NJ), used for MRI imaging of the central nervous system, is desirable for producing magnetic carrier due to its biocompatibility, chemical stability and high molar susceptibility. CTV measurements of non-magnetic polystyrene microspheres (PSMs) in dilute Gd^{3+} solution, confirm the predicted effects and serve as a basis to validate the assumptions of magnetic particle tracking. QMS studies of red blood cells (RBCs)

and PSMs show that crossover is significantly reduced by the addition of Gd^{3+} to the carrier medium. This allows selection of flow conditions to yield greater throughput, purity and resolving power.

METHODS: A thorough description of the fluid dynamic and magnetic theory applicable to the QMS is given [1]. The separation element of the QMS lies in the annulus between a coaxial core rod 2, and an outer cylinder 3, as illustrated in Fig 1. This is surrounded by four pole pieces 1, generating a magnetic quadrupole field. Coaxial cylindrical splitters 4, separate inlet and outlet streams, where the feed and carrier streams are a' and b' , and depleted and enriched streams are a and b . Three or four independent syringe drives control the flow components. The source of the magnetomotive force is four Nd-Fe-B permanent magnets.

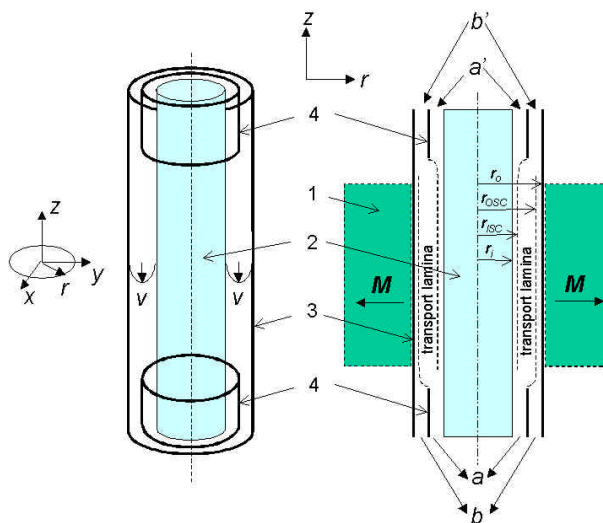


Fig. 1: Perspective view not showing magnet (left) and axial section (right) of QMS.

The component flows converge just beyond the inlet splitter, and the virtual boundary separating the fluids and extending down the column, is called the inlet splitting surface (ISS); see Fig. 1. The radial position of the ISS depends non-linearly on the ratio of the feed component flow to the total flow, Q_a/Q :

$$\frac{Q_a}{Q} = \frac{[2r^2 - r^4 + 2A_2r^2 \ln r - A_2r^2]_{r_i}^{r_{ISS}}}{A_1(1 - r_i^2)} \quad (1)$$

A_1 and A_2 are constants which depend on the channel geometry, \tilde{n} is the dimensionless ratio r/r_o , r_o is the radial distance to the inside surface of the cylinder, and \tilde{n}_i is defined at the core rod radius r_i . A similar outlet splitting surface (OSS) extends upward from the outlet splitter and separates the flow components a and b . Analogously to eq. 1, the position of the OSS, \tilde{n}_{OSS} depends on Q_a/Q . The transport lamina thickness, d , is the distance between the splitting surfaces, OSS and ISS.

The numerical values of the QMS parameters are maximum field, $B_o = 1.344$ T, $r_o = 4.53$ mm, $r_i = 2.38$ mm, inlet flow rate ratio, $Q_a/Q = 0.2$, variable outlet flow rate ratio, $Q_a/Q = 0.1 \dots 0.35$, and total flow rate, $Q = 4$ ml/min.

Magnetically labeled cells in a magnetic field experience a magnetic drift velocity, $u_m = mS_m$, where m is the cell magnetophoretic mobility and S_m is the field strength parameter. In the general case, and applicable to the field of CTV, S_m is described for a particle of inducible magnetization, as

$$S_m = \frac{|\nabla B^2|}{2\mathbf{m}_0} \quad (2)$$

where \mathbf{m}_0 is the permeability of free space. In the ideal quadrupole system, S_m is related to the system parameters by:

$$S_m = \frac{B_o^2}{\mathbf{m}_0 r_o} \frac{r}{r_o} \quad (3)$$

B_o , in this case, is the flux density at the inner surface of the outer cylinder, r_o . Note that S_m depends on the radius r , but not on the angular coordinate, ϑ . The mobility is independent of the magnetic environment and relates to properties of the cell, label and medium by:

$$m = \frac{2}{9} \frac{R^2 \Delta c}{\zeta \mathbf{h}} \quad (4)$$

R is the particle radius, ζ is the medium viscosity and Δc is the difference between the volumetric susceptibilities of the cell and the medium. Neglecting the slight contribution of water, the volumetric susceptibility of a gadolinium solution, in SI units, is:

$$c = \frac{4p}{1000} [Gd^{3+}] c_{M,Gd^{3+}}^{CGS} \quad (5)$$

where $c_{M,Gd^{3+}}^{CGS}$ is the molar susceptibility of Gd^{3+} in CGS units, 0.027. For an unlabeled cell or non-magnetic particle of approximately zero susceptibility, suspended in a Gd^{3+} solution, eqs. 4 and 5 become:

$$mh = -\frac{8p}{9000} R^2 c_{M,Gd^{3+}}^{CGS} [Gd^{3+}] \quad (6)$$

It is clear that a plot of mh vs. $[Gd^{3+}]$ should yield a straight line of slope given by the constant parameters.

CTV, a device for measuring the mobility of cell or particle suspensions, comprises a permanent magnet circuit with pole pieces shaped to produce a nearly constant S_m within the field of view of a microscope [3]. The induced magnetic particle velocity u_m is, therefore, constant for paramagnetic particles. The CTV analysis area is 1.27 x 1.72 mm. Assuming that a uniform probability distribution governs the uncertainty of positioning the viewing area in the magnetic field, the weighted mean of the horizontal component of $\tilde{N}B^2$ is 376.8 ± 2.5 T²/m, giving rise to a mean S_m of 1.499×10^8 TA/m².

A microscope with a mounted CCD camera with a frame speed of 30 Hz, is used to observe particle migrations in a glass channel in the magnetic field. A μ -Tech Frame Grabber is used to convert the analog camera image into a binary 480x640 pixel array, where each pixel contains eight bits of gray-level. To improve low-mobility sensitivity, frame speeds less than 30 Hz are used by selectively skipping frames during the acquisition. The particle tracking and velocity calculation is performed using a computer algorithm consisting of two parts: determination of particle location and 2-D tracking. The output of CTV gives location and velocity data, for multiple particles, over the observed frames. These velocities, combined with the known S_m , give mobilities. Typically, hundreds of particles are analyzed in a sample, enabling the construction of mobility histograms and the calculation of population statistics.

The CTV computational algorithm has been tested for self-consistency and sensitivity by tracking the sedimentation of polystyrene microspheres. Validation of the magnetic assumptions has been explored by tracking magnetite-coated polystyrene

beads, which were separately measured with a magnetometer [4]. The results were affected by the large degree of dispersion of magnetite content and the non-constant velocities of ferromagnetic materials in the field of the CTV magnet. An improved method of validation, described below, applies to the tracking of monodisperse PSMs suspended in a solution of paramagnetic salt, in which the expected direction of migration opposes the field gradient.

RESULTS & DISCUSSION: Figure 2 gives distributions, obtained by CTV, for monodisperse PSMs of diameter $6.992 \pm 0.050 \mu\text{m}$ (Duke Scientific Corp., Palo Alto, CA) suspended in various dilutions of MAGNEVIST®, expressed as the concentration of Gd^{3+} . The abscissa combines mobility with medium viscosity, whose dependence on contrast agent concentration was determined with a plate-and-cone viscometer. The peak relative dispersions remain fairly constant, and the control peak is statistically distinct from that of the lowest concentration. Fig. 3 gives the experimental data and theoretical plot of $m\eta$ versus $[\text{Gd}^{3+}]$, with the aid of eq. 6. The data from Fig. 2 are plotted with regression line and confidence interval. Because the regression line fits the measured data with a high degree of confidence, the disparity with the theoretical curve indicates that an unknown systematic error may be involved. Nonetheless, the slopes compare favorably: -8.195×10^{-16} (regression) compared with -9.215×10^{-16} (theoretical).

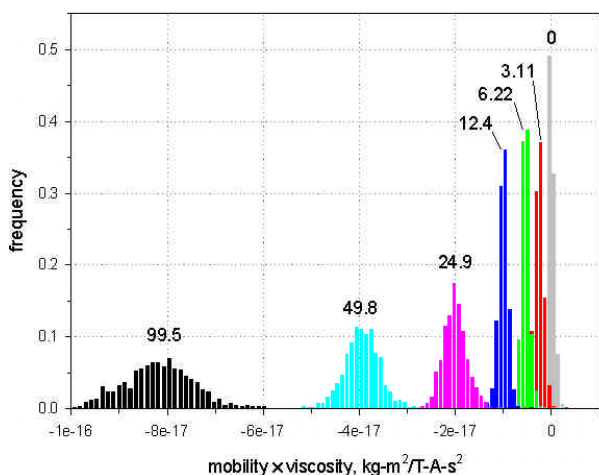


Fig. 2: CTV analyses of monodisperse PSMs suspended in various millimolar concentrations of Gd^{3+} .

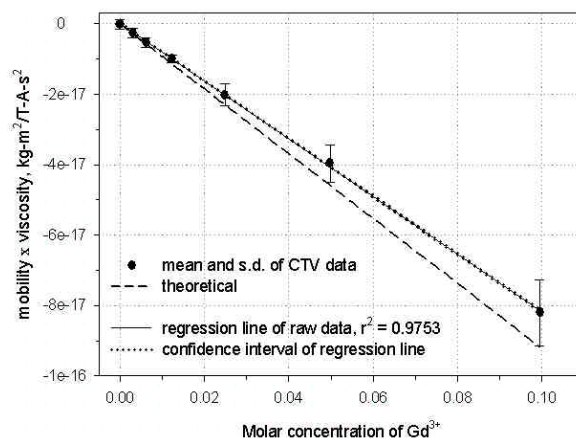


Fig. 3: Data reduction of PSMs in Gd^{3+} medium.

The non-specific crossover of $15.8 \mu\text{m}$ PSMs in the QMS was investigated, as shown in Fig. 4. Data were obtained by injecting 3-5 samples into the column, for each flow condition, and monitoring the light attenuation with a UV detector at outlet b, as described [2]. The dashed line shows the position of the ISS relative to the core rod and outer wall of the channel. The ISS is calculated for a constant inlet flow rate ratio of 0.2, with the use of eq. 1. The outlet flow rate ratios Q_a/Q were varied, corresponding to various positions of the OSS and transport lamina thicknesses given on the abscissa. Under control conditions the particles have no significant magnetization relative to the medium (0.5% fetal bovine serum in Plasmalyte™ (Baxter Healthcare, Deerfield, IL). And under ideal behavior - no geometric imperfections or external forces - their fractional recovery F_b , at and beyond the ISS, must be zero.

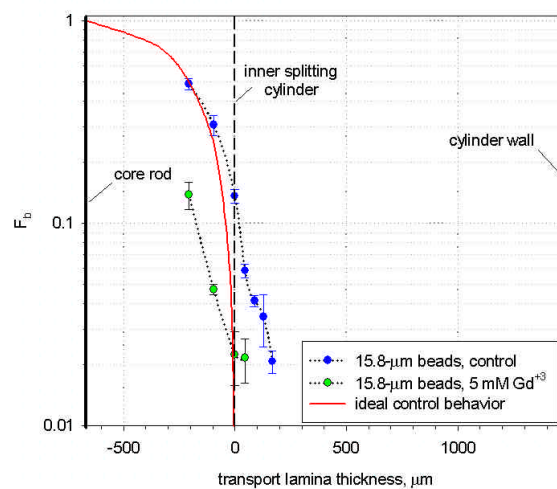


Fig. 4: The crossover PSMs in the QMS. Bold lines of the core rod and cylinder wall bound the annulus.

The ideal control curve is generated by the simple relationship, $F_b = 1 - Q_a/Q_a'$, with Q_a ranging from 0 to Q_a' . Evidence of non-ideal behavior is seen by the non-zero recoveries at positive transport lamina.

For a practical QMS separation, a suitable outlet flow rate ratio is found from the transport lamina which meets a low crossover criterion, e.g. 2%. If this criterion can be satisfied while reducing the outlet flow rate ratio, theoretically, the resolving power and recovery can be improved. Likewise, reducing crossover for the same outlet flow rate ratio improves the purity in the enriched fraction. Either aim might be achieved when gadolinium salt is added to the medium, as seen in Fig. 4.

These experiments were repeated with red blood cells (RBC's) replacing PSMs; Fig. 5. RBCs, whose mean hydrodynamic diameter is 5.52 μm , are important in that they are a frequent contaminant in leukocyte separations involving human blood, bone marrow and apheresis product. Comparison of Fig. 5 with Fig. 4 gives evidence that RBCs have a higher crossover, under the same conditions, than PSMs, probably due to the bi-concave shape of the RBCs. Further, the effect of 5 mM Gd^{3+} in reducing crossover is greater for the PSMs, because of the effect of size in eq. 3. Still, the possibility of adding gadolinium salt to the medium in practical separations of leukocytes is indicated.

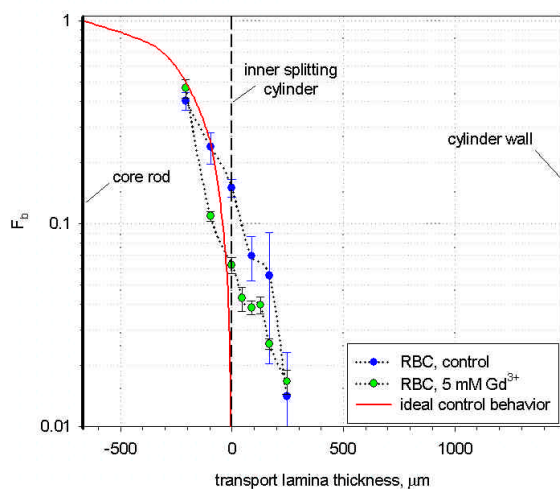


Fig. 5: The crossover of RBCs in the QMS.

REFERENCES: ¹P.S. Williams, M. Zborowski, and J.J. Chalmers (1999) *Flow rate optimization for the quadrupole magnetic cell sorter*, Analytical Chemistry **71**: 3799-3807. ²M. Hoyos, L.R. Moore, K.E. McCloskey, S. Margel, M. Zuberi, J.J. Chalmers, and M. Zborowski (2000) *Study of magnetic particles pulse-injected into an annular*

SPLITT-like channel inside a quadrupole magnetic field, J Chromatography A **903**: 99-116. ³J.J. Chalmers, Y. Zhao, M. Nakamura, K. Melnik, L. Lasky, L. Moore, and M. Zborowski (1999) *An instrument to determine the magnetophoretic mobility of labeled, biological cells and paramagnetic particles*, J Magnetism and Magnetic Materials **194**: 231-241. ⁴L.R. Moore, M. Zborowski, M. Nakamura, K.E. McCloskey, S. Gura, M. Zuberi, S. Margel, and J.J. Chalmers (2000) *The use of magnetite-doped polymeric microspheres in calibrating cell tracking velocimetry*, J Biochem Biophys Methods **44**: 115-130.

ACKNOWLEDGMENTS: These studies were supported by the grants from the NIH (R01 CA62349 to M.Z., R33 CA81662 to J.J.C.), and the NSF (BES-9731059 to J.J.C. and M.Z.). The RBC specimens were provided by Dr. G. Oстера, National Institute of Diabetes, Digestive and Kidney Disease, NIH, Bethesda, MD.